

The compact object of HESS J1731-347 and its implication on neutron star matter

Prasanta Char^{1,2}, Bhaskar Biswas³

¹*Departamento de Física Fundamental, Universidad de Salamanca, Plaza de la Merced S/N, 37008 Salamanca, Spain,*

²*Space Sciences, Technologies and Astrophysics Research (STAR) Institute, Université de Liège, Bât. B5a, 4000 Liège, Belgium,*

³*Hamburger Sternwarte, Gojenbergsweg 112, D-21029 Hamburg, Germany*

In this work, we investigate the impact of the possibility of a small, subsolar mass compact star, such as the recently reported central compact object of HESS J1731-347, on the equation of state (EOS) of neutron stars. We have used a hybrid approach to the nuclear EOS developed recently where the matter around nuclear saturation density is described by a parametric expansion in terms of nuclear empirical parameters and represented in an agnostic way at higher density using piecewise polytropes. We have incorporated the inputs provided by the latest neutron skin measurement experiments from PREX-II and CREX, simultaneous mass-radius measurements of pulsars PSR J0030+0451 and PSR J0740+6620, and the gravitational wave events GW170817 and GW190425. The main results of the study show the effect of HESS J1731-347 on the nuclear parameters and neutron star observables. Our analysis yields the slope of symmetry energy $L = 45.71^{+38.18}_{-22.11}$ MeV, the radius of a $1.4M_{\odot}$ star, $R_{1.4} = 12.18^{+0.71}_{-0.88}$ km, and the maximum mass of a static star, $M_{\max} = 2.14^{+0.26}_{-0.17}M_{\odot}$ within 90% confidence interval, respectively.

I. INTRODUCTION

Recent observation of a compact object inside the supernova remnant HESS J1731-347 has provided an estimation of its mass and radius to be $M = 0.77^{+0.20}_{-0.17}M_{\odot}$ and $R = 10.4^{+0.86}_{-0.78}$ km at 1σ credible levels, respectively [1]. Understandably, this observation has generated a lot of attention from the nuclear physics community working on the dense matter physics beyond the normal nuclear matter density [2–7]. Different possibilities have been explored to characterize this object, such as, a strange quark or a hybrid star [8–13], or a dark matter admixed compact star [14]. A typical neutron star (NS) usually has a mass within the range of $\sim 1 - 2M_{\odot}$. NSs being extremely dense compact objects have profound effects on our understanding of dense nuclear matter higher than nuclear saturation density (ρ_0) [15]. Usually, the equation of state (EOS) of highly dense matter is connected to the observations of the masses and radii of the compact objects through the solutions of the TOV equations. Hence, each new source with observed mass and radius allows us to test and constrain our models of nuclear physics and increase precision over the previous results. Therefore, the compact object of HESS J1731-347 being an outlier in the distribution of observed pulsar masses may provide a unique insight to neutron star matter. However, one must take this estimation with caution as other studies have indicated several assumptions on the atmospheric composition and distance that may have led to these extreme numbers [16]. In any case, this situation provides an opportunity to check the consistency of such extreme observations with our existing models of neutron star matter, if they are really confirmed in the future.

Our understanding of NS matter and the nuclear equation of state (EOS) have improved drastically after the several astrophysical observations in the previous decades, such as the massive pulsars ($\gtrsim 2M_{\odot}$) [17–

19], and the first ever observation of gravitational waves (GW) and the electromagnetic counterparts from the binary neutron star merger event GW170817, reported by the LIGO-Virgo-Kagra (LVK) collaboration [20, 21]. The GW observation has provided important information on the combined tidal deformability of the binary system which is an EOS-dependent quantity. Then, the NICER collaboration has also provided simultaneous mass-radius measurements of PSR J0030+0451 and PSR J0740+6620 [22–25]. From the perspective of ground-based experiments, the measurements of neutron skin thickness of ^{208}Pb by PREX [26] and ^{48}Ca by CREX [27] collaborations, respectively, have shed a new light on the nuclear symmetry energy and its slope parameter. In parallel, there have also been advancements in the ab-initio calculations of the properties of pure neutron matter with chiral effective field theories [28–34]. These calculations have provided major insights to the properties of nuclear matter around and below nuclear saturation.

In this paper, we investigate the influence of the PREX, and CREX measurements on the EOS, along with the mass-radius data of HESS J1731-347, assuming it to be a neutron star. We introduce these constraints successively and check their effects on the nuclear matter properties. The paper is organized in the following way. In section II, we briefly describe our EOS model. The relevant constraints used in the work and the Bayesian methodology are discussed in section III. Finally, we discuss our findings in section IV and summarize in section V.

II. EOS OF NS MATTER

In this section, we provide a brief overview of our approach to model the supranuclear matter inside the NS. We have used the hybrid+PP EOS parametrization that has been developed by Biswas *et al.* [35] and used to pro-

vide multimessenger analyses of NS properties [36, 37]. It has also been used to create a framework to infer Hubble parameter directly from GW signals from the future BNS mergers [38, 39]. The core EOS consists of two main parts: a) nuclear physics informed expansion-based near saturation, b) agnostic polytropic at high densities. Around ρ_0 , we have used an EOS based on Taylor's series expansion of the isoscalar and isovector components of the energy per nucleon.

First the energy per particle is expanded in terms of asymmetry upto second order.

$$e(\rho, \delta) \approx e_0(\rho) + e_{\text{sym}}(\rho)\delta^2, \quad (1)$$

where, $e_0(\rho)$ is the energy per particle for symmetric nuclear matter (SNM), and $e_{\text{sym}}(\rho)$ is the symmetry energy. At ρ_0 , they are further expanded in Taylor's series and the coefficients are defined as the nuclear empirical parameters.

$$e_0(\rho) = e_0(\rho_0) + \frac{K_0}{2}\chi^2 + \dots, \quad (2)$$

$$e_{\text{sym}}(\rho) = e_{\text{sym}}(\rho_0) + L\chi + \frac{K_{\text{sym}}}{2}\chi^2 \dots, \quad (3)$$

where $\chi \equiv (\rho - \rho_0)/3\rho_0$ expresses the deviation from ρ_0 . We keep the terms upto second order as the higher order terms do not contribute significantly to the EOS around ρ_0 . We also fix the saturation density, $\rho_0 = 0.16 \text{ fm}^{-3}$ and binding energy per nucleon of SNM at saturation, $e_0(\rho_0) = -15.9 \text{ MeV}$ [40–42]. Therefore the free parameters in this model are the incompressibility (K_0), nuclear symmetry energy (e_{sym}) and its slope parameter (L), and the isovector incompressibility (K_{sym}) at saturation. We consider the previous theoretical and experimental works to estimate these quantities [43–45] and take a uniform prior over a large range of value to incorporate their uncertainties. For the cold NS matter, the additional conditions of β -equilibrium and charge neutrality are also imposed. Then, at higher densities we have used an agnostic EOS with piecewise polytrope (PP) parametrization [46]. In particular, we have used an arrangement with a three-segment polytrope ($\Gamma_1, \Gamma_2, \Gamma_3$ being the polytropic indices) starting at $1.25\rho_0$. The next two stitching points are 1.8 and $3.6\rho_0$, respectively. Hence, we have a total of seven parameters, $\mathcal{E} = \{K_0, e_{\text{sym}}, L, K_{\text{sym}}, \Gamma_1, \Gamma_2, \Gamma_3\}$, representing the EOS of NS matter. For the crust EOS, we have used the standard Baym-Pethick-Sutherland EOS table [47].

III. METHODOLOGY

In this section, we describe briefly the inference methodology used in this work. We have used the tidal deformability posteriors from two BNS merger events GW1701817, and GW190425 [48–51]. We have used the mass-radius posteriors of PSR J0030+0451 and PSR

J0740+6620 [52–55]. For the HESS J1731-347, we have used the M-R posterior [56] assuming the uniformly emitting carbon atmosphere provided by Doroshenko *et al.* [1]. The posterior of the EOS parameters can be expressed as,

$$P(\mathcal{E}|d) \propto \Pi_i P(d_i|\mathcal{E})P(\mathcal{E}), \quad (4)$$

where $d = (d_{\text{LVK}}, d_{\text{NICER}}, d_{\text{HESS}}, d_{\text{PREX}}, d_{\text{CREX}})$ is the set of different constraints used. The individual likelihoods can be written as follows:

- GW Observations: the masses m_1, m_2 of the two binary components and the corresponding tidal deformabilities Λ_1, Λ_2 . In this case,

$$P(d_{\text{LVK}}|\mathcal{E}) = \int_{m_2}^{m_{\text{max}}} dm_1 \int_{m_{\text{min}}}^{m_1} dm_2 P(m_1, m_2|\mathcal{E}) \times P(d_{\text{LVK}}|m_1, m_2, \Lambda_1(m_1, \mathcal{E}), \Lambda_2(m_2, \mathcal{E})), \quad (5)$$

where m_{max} is the maximum mass of a NS for a particular set of EOS parameter \mathcal{E} , $P(m_1, m_2|\mathcal{E})$ is the prior distribution over the component masses at the source frame. This is determined by the population modelling of NSs.

$$P(m_1, m_2|\mathcal{E}) = P(m_1|\mathcal{E}) \times P(m_2|\mathcal{E}) \quad (6)$$

We take a simple population model define by,

$$P(m | \mathcal{E}) = \begin{cases} \frac{1}{m_{\text{max}}(\mathcal{E}) - m_{\text{min}}}, & \text{iff } m_{\text{min}} \leq m \leq m_{\text{max}} \\ 0, & \text{otherwise,} \end{cases} \quad (7)$$

where we have chosen, $m_{\text{min}} = 0.1M_{\odot}$ in our analyses. Given the high-precision measurement of the chirp mass in GW observations, equation 5 can be further simplified by fixing the GW chirp mass to its median value with not so much affecting the result [57] given its high precision measurement. Then we will have one less parameter to integrate over as m_2 will be a deterministic function of m_1 . Hence, we fix it to the observed median value and use it to generate a set of binary neutron star systems and their respective tidal deformability. Then, we evaluate the likelihood directly from the GW data with the help of a Gaussian kernel density estimator (KDE). We have used the publicly available posterior samples of $m_1, m_2, \Lambda_1, \Lambda_2$ distribution of GW170817¹ and GW190425².

- X-ray observations: the mass (m) and radius (R) measurements of NS. Therefore, the corresponding

¹ LVK collaboration, <https://dcc.ligo.org/LIGO-P1800115/public>

² LVK collaboration, <https://dcc.ligo.org/LIGO-P2000026/public>

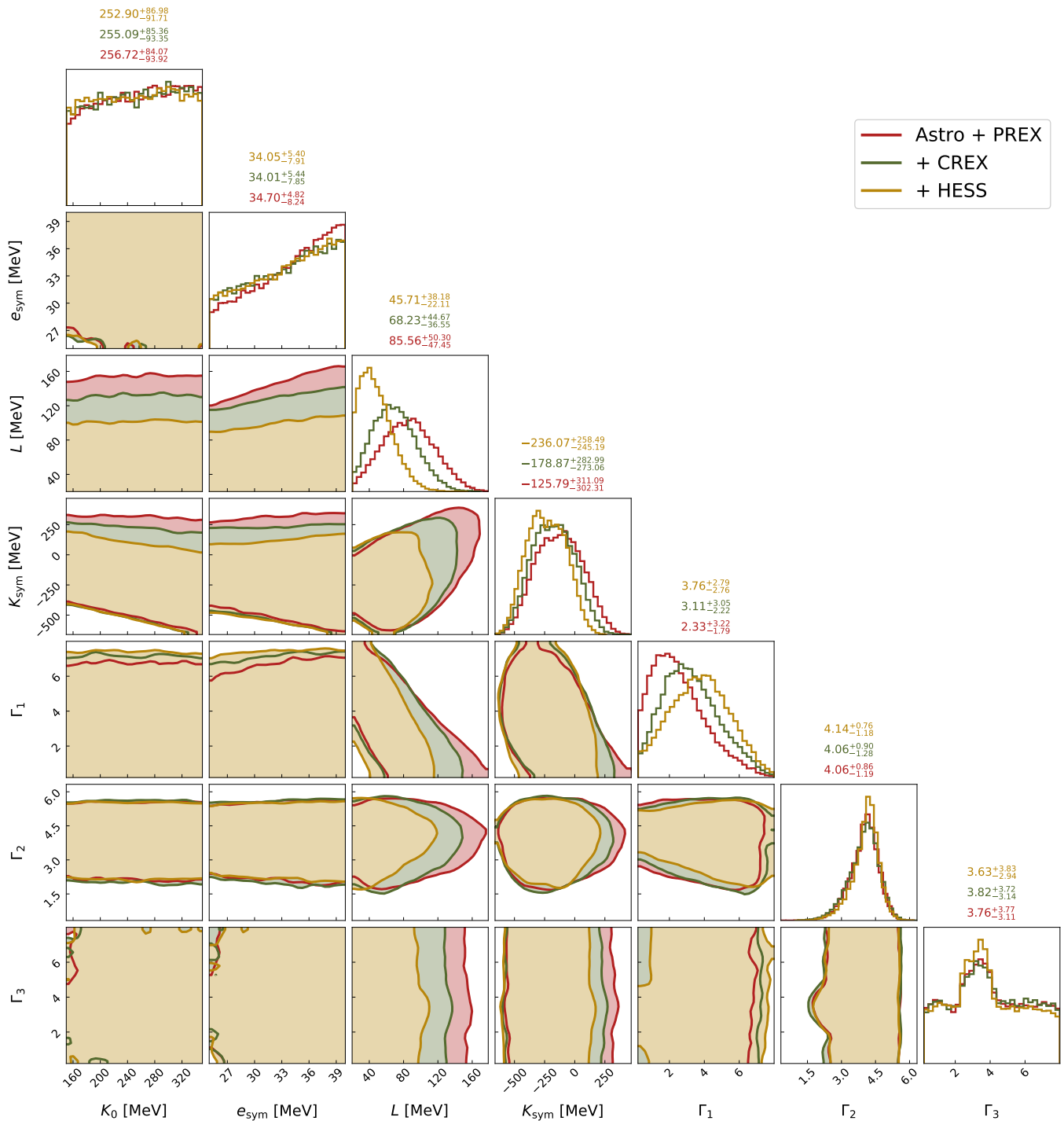


FIG. 1. Posterior distribution of EOS parameters with their 90% CI.

likelihood takes the following form,

$$P(d_{X\text{-ray}}|\mathcal{E}) = \int_{m_{\min}}^{m_{\max}} dm P(m|\mathcal{E}) P(d_{X\text{-ray}}|m, R(m, \mathcal{E})). \quad (8)$$

Similar to GW observations, we modelled the likelihood for X-ray with Gaussian KDEs.

- Neutron skin thickness measurements: PREX collaboration reported the neutron skin thickness of ^{208}Pb to be $R_{\text{skin}}^{208} = 0.283 \pm 0.071$ fm. CREX collaboration reported the neutron skin thickness of ^{48}Ca to be $R_{\text{skin}}^{48} = 0.121 \pm 0.026(\text{exp}) \pm 0.024(\text{model})$ fm.

As in Ref. [37, 58], we have used a universal relation between r_{skin} and empirical parameter L pro-

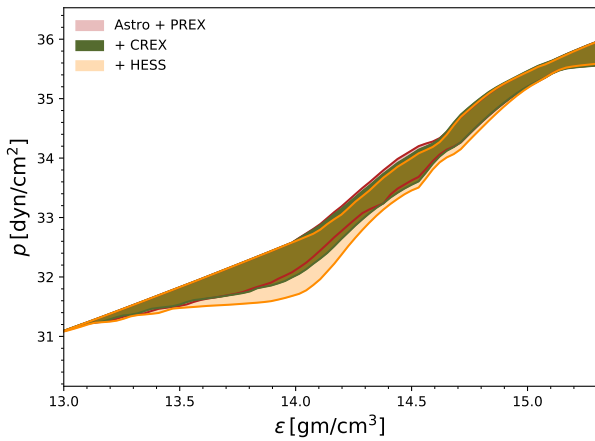


FIG. 2. Posterior distribution of pressure as a function of energy density at 90 % CI. The axes are shown in the logarithmic scale.

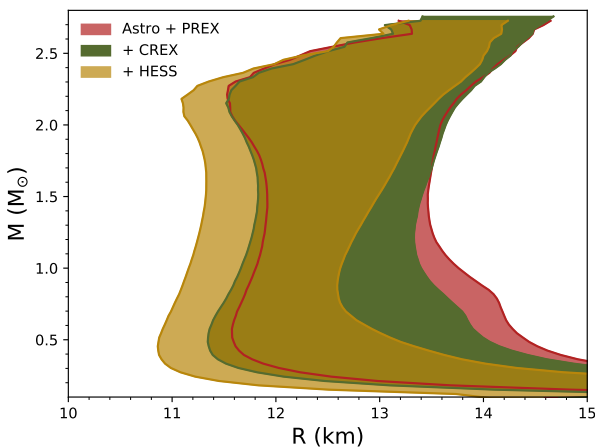


FIG. 3. Mass-radius posteriors at 90 % CI with the EOS models shown in figure 2.

posed in Ref. [59] for the likelihood computation of PREX-II:

$$R_{\text{skin}}^{208}[\text{fm}] = 0.101 + 0.00147 \times L[\text{MeV}]. \quad (9)$$

Similarly for CREX, we also use a similar empirical relation from Ref. [60], to evaluate the neutron skin thickness of ^{48}Ca .

$$R_{\text{skin}}^{48} = 0.0416 + 0.6169 R_{\text{skin}}^{208}. \quad (10)$$

Finally, we use a Gaussian distribution to model their likelihood.

IV. RESULTS

In this paper, we focus on three different analyses with different combinations of astrophysical constraints and

Parameter	Prior
K_0 (MeV)	$\mathcal{U}(150, 350)$
e_{sym} (MeV)	$\mathcal{U}(25, 40)$
L (MeV)	$\mathcal{U}(20, 180)$
K_{sym} (MeV)	$\mathcal{U}(-1000, 500)$
Γ_1	$\mathcal{U}(0.2, 8)$
Γ_2	$\mathcal{U}(0.2, 8)$
Γ_3	$\mathcal{U}(0.2, 8)$

TABLE I. Prior distributions of the EOS parameters

information from the neutron skin measurement experiments. First, we conduct a study with the GW170817, GW190425, two NICER measurements, and PREX results. This is similar to the study done in [37]. We have used different priors and looked for any effect on the EOS quantities. Then, we have added the information from CREX, and finally the M-R data of the HESS J1731-347.

In Figure 1, we have shown the posterior distributions of the EOS parameters along with their median and 90% confidence intervals (CI) for different constraints applied. We denote the GW and NICER as Astro, then our first case is “Astro + PREX”. The second case has CREX on top of the first case, denoted by “+ CREX”. Finally, the third case includes HESS J1731-347 along with the first two, denoted by “+ HESS”. We find that K_0 and e_{sym} are not constrained by the astrophysical data used. The distribution of K_0 is mostly flat, whereas the we see an increasing trend for e_{sym} to the higher values. This is a result of choosing a flat prior on these two quantities. In the previous work within the same EOS model [35, 37], similar trends were seen when uniform priors were used. Also, when Gaussian priors were used, the posterior reflected the priors again confirming that these parameters are insensitive to astrophysical constraints and the PREX measurements. Here, we confirm again that the CREX and HESS measurements have no effect on K_0 and e_{sym} . However, the situation is different when we look at L and K_{sym} . Taking a Gaussian prior of $\mathcal{N}(58.7, 28.1)$ MeV on L , its bound was estimated in Ref. [37] to be, $L = 54^{+21}_{-20}$ MeV with astrophysical constraints, and $L = 69^{+21}_{-19}$ MeV at 1σ level after adding the PREX-II result. In our case, we have used a large uniform and found the median value shifted to a higher value, $L = 87^{+50}_{-47}$ MeV. Higher L values were reported previously as a consequence of the PREX measurements [61, 62]. Then, we see the median of L getting shifted to lower values after successively adding CREX and HESS J1731-347. After applying all the constraints, we find, $L = 46^{+38}_{-22}$ MeV. From nuclear experiments, there is not much known about K_{sym} . In the literature, its value is suggested to be negative. The constraints on K_{sym} from astrophysics is also weak as we found that the 90% CI is quite large for all cases, but we see the similar trend in the median value, as L . With Astro+PREX, we find the

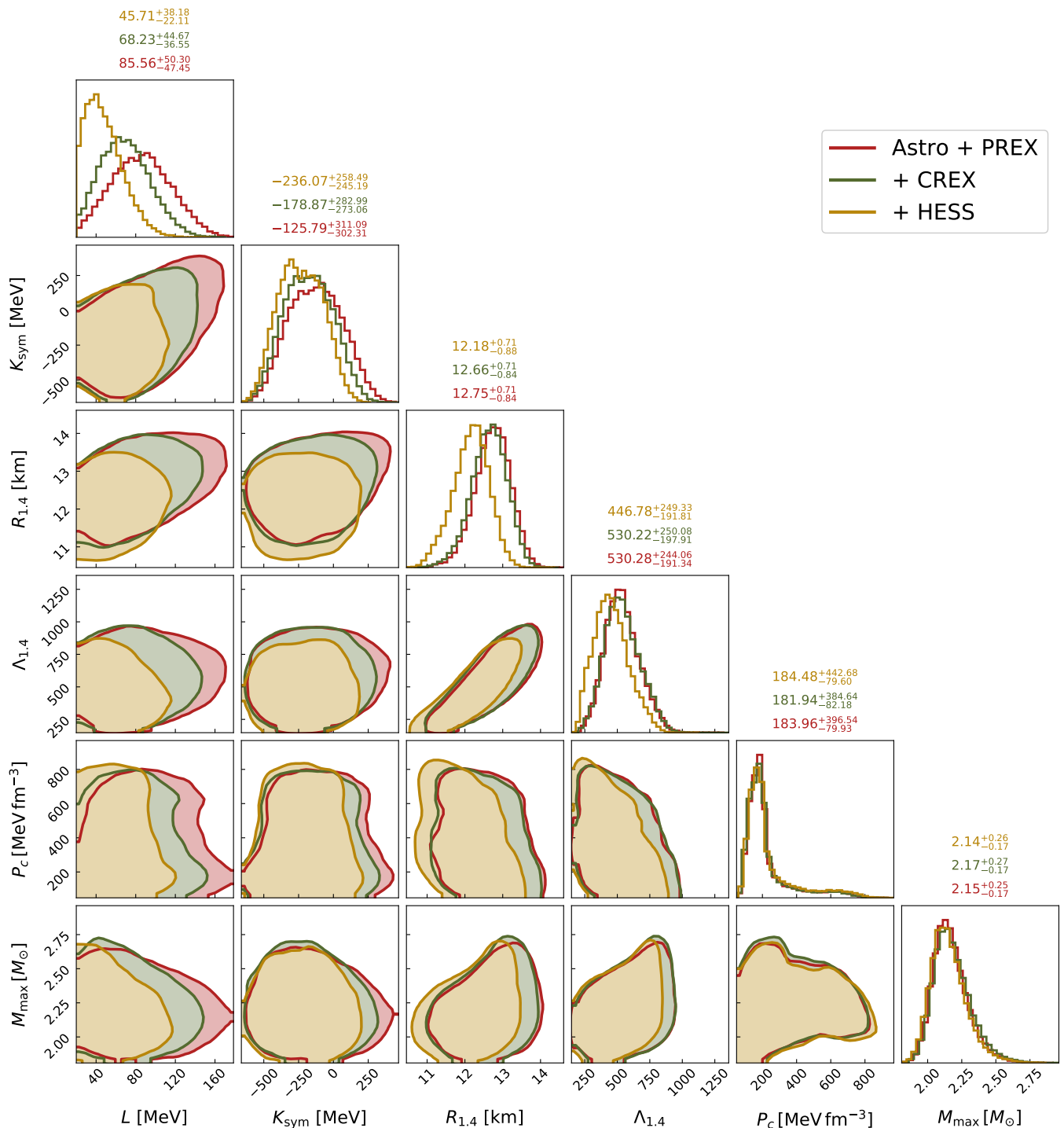


FIG. 4. Correlation plot for isovector quantities with neutron star observables with their 90% CI.

median of K_{sym} to be about -126 MeV which shifts to lower values of -179 MeV after adding CREX and further down to be -236 MeV after adding HESS. We also notice a correlation between L and K_{sym} . Regarding the piecewise polytropes at higher densities, we only see the changes in first polytrope, Γ_1 which gradually increases with additional constraints. Similar correlation were also

found by Refs. [63, 64] using a semiagnostic EOS model. The only significant correlation among the EOS parameters we see, is between L and Γ_1 . The interplay between these two parameters is seen in the pressure-vs-energy density plot in Figure 2. We observe that the inclusion of HESS makes the EOS softer at lower densities to produce smaller radii for the NS sequences by the decrease

□

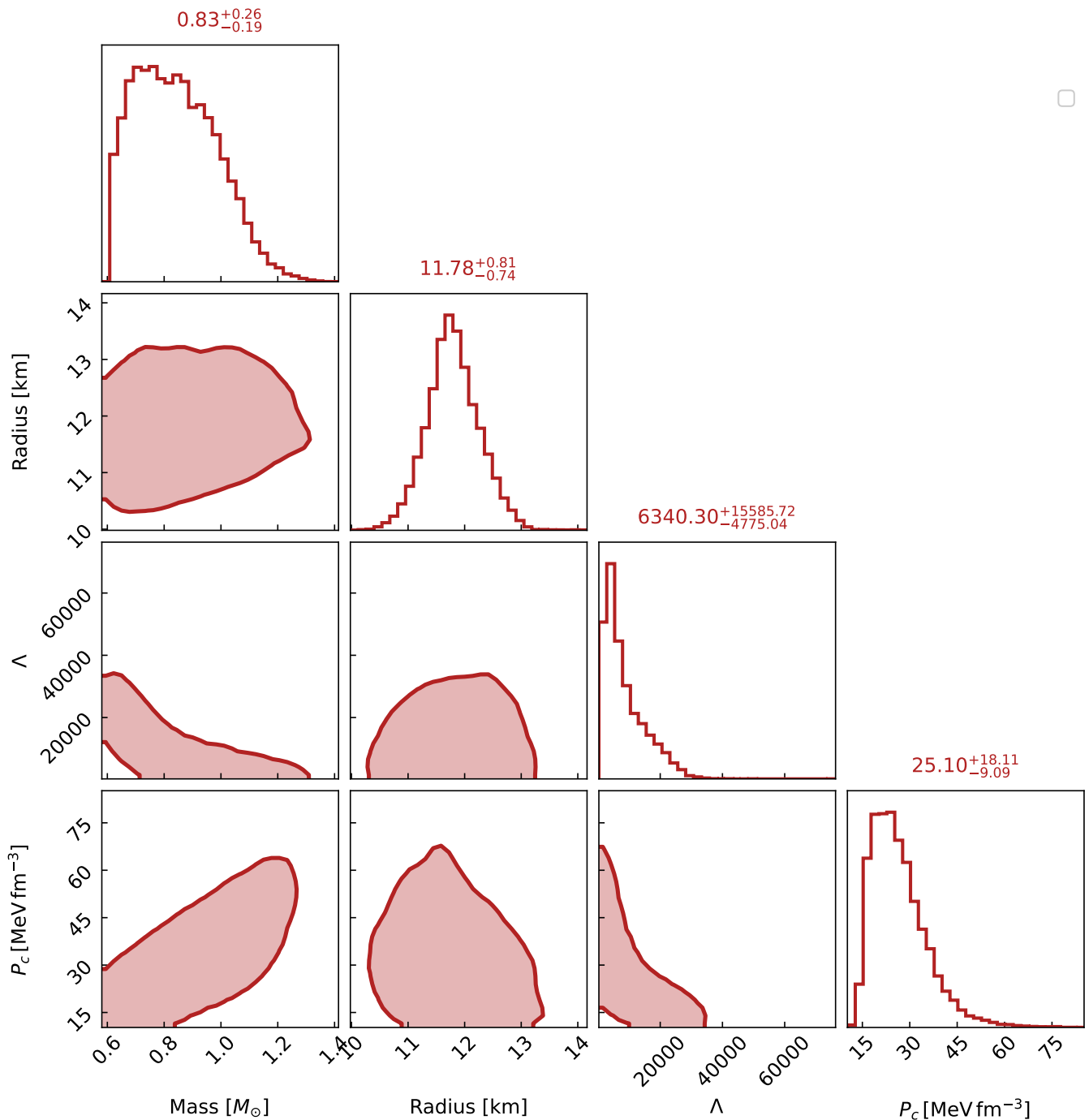


FIG. 5. Correlation plot of inferred properties of HESS J1731-347 at 90% CI.

of the slope of symmetry energy. But, the requirement of $\sim 2M_{\odot}$ makes the EOS stiffer at high density thereby increasing the first polytrope. The absolute maximum masses from these EOSs stay unaffected because of no significant changes in Γ_2 and Γ_3 .

In Figure 3, we have shown the mass-radius posterior of the three cases corresponding to the EOS posteriors, shown in Figure 2. Here, we can clearly see the effect of

the constraints on the structure of the NSs. The maximum mass regions for these constraints remain mostly unchanged following the same trend in the EOS posteriors. But, the radii of the low mass stars become gradually smaller with the addition of CREX and HESS. This is consistent with the decrease of the slope of symmetry energy at saturation in Figure 1.

The correlations among the astrophysical observables

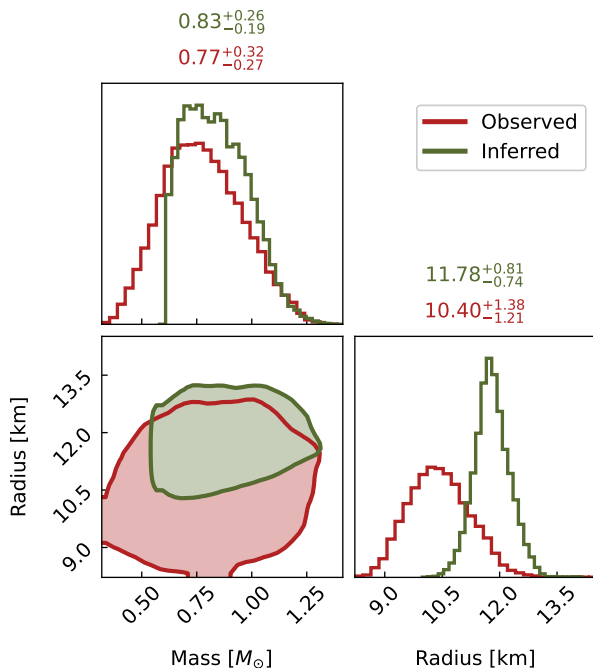


FIG. 6. Comparison between the actual data and inferred mass-radius posteriors of HESS J1731-347 at their 90% CI.

($R_{1.4}$, $\Lambda_{1.4}$, M_{\max}) and the nuclear parameters are shown in figure 4. Here, we show only L and K_{sym} among the nuclear parameters as we have seen from figure 1, these are the ones most affected by the constraints. We also predict the central densities of the maximum mass stars from our analysis. With Astro+PREX, we get the maximum mass $\sim 2.15M_{\odot}$ with the central pressure ~ 184 MeV fm $^{-3}$. After adding CREX, we see a slight increase in the maximum to $\sim 2.17M_{\odot}$, indicating slight stiffness at that densities. As a result, the central pressure decreases slightly to ~ 182 MeV fm $^{-3}$. However, the radius of $1.4M_{\odot}$ NS, $R_{1.4}$ behaves in an opposite way. We find that including CREX reduces $R_{1.4}$ from ~ 12.75 km to ~ 12.66 km, thereby indicating a softness around that densities. Although the change in the tidal deformabilities is negligible. Before adding HESS, the $\Lambda_{1.4}$ remains around ~ 530 , consistent with the findings of Ref. [37]. Finally, the addition of HESS decreases both $R_{1.4}$, $\Lambda_{1.4}$ and M_{\max} . While the decrease in M_{\max} is very small, to $\sim 2.14M_{\odot}$, the $R_{1.4}$ becomes ~ 12.2 km. The tidal deformability decreases to ~ 447 . We can comment that the softening due to HESS occurs over the whole range of densities, small at very high densities, but significant at lower densities. This is again consistent from the behavior of L . In figure 4, we see a hint of correlation of L with $R_{1.4}$, but not with M_{\max} . This type of correlation was also seen in previous studies [65] where a relativistic hadronic model was used.

Now, we discuss the properties of HESS J1731-347 calculated within the hybrid+PP model. In figure 5, we have shown the inferred mass, radius, tidal deformabil-

ity, and central pressure within 90% CI. We infer its mass $0.83^{+0.26}_{-0.19} M_{\odot}$ and radius $11.78^{+0.81}_{-0.74}$ km. Since it is a relatively smaller object, its median of tidal deformability (~ 6340) is on the higher side. We also estimate its central pressure to be $25.10^{+18.11}_{-9.09}$ MeV fm $^{-3}$. This corresponds to a slightly higher pressure than the value of pressure at saturation. In figure 6, we compare the observed M-R data against the inferred values in this work. Although, we have found an overlap at 90% CI, the radii do not overlap at 68% CI. We also see a sharp bound on the lower bound on the inferred mass. This is a physical bound signifying that it is not possible to build a lower mass configuration beyond that region within our nucleonic EOS model that satisfies the constraint on the radius simultaneously. This is the limit of the hybrid+PP model on the low mass, low radius side. If we observe a new object even smaller than this object both in its size and mass, we have to invoke a different hypothesis regarding the composition of such object.

V. CONCLUSION

In this work, we have presented a full statistical analysis of the impact of the mass-radius measurements of the central compact object of HESS J1731-347 on NS matter consisting of nucleons. We have used the full M-R posterior of HESS J1731-347 while performing the Bayesian analysis. We have also shown how the neutron skin thickness measurements affect NS observables. We have systematically studied the effect of the combinations of these constraints on the symmetry energy and its derivatives (L and K_{sym}). We have found the inferred EOS posterior becomes stiffer due to the effect of PREX, but becomes substantially softer with HESS. The softening is more prominent at lower densities than at higher densities as the maximum mass remains mostly unchanged. We have to keep in mind the systematic uncertainties in the modelling of X-ray spectra from HESS J1731-347, as mentioned in several works [6, 16]. Given such a star exists, we have found that this measurement can push our EOS model to its limit.

While we were conducting this study, a new simultaneous mass-radius measurement of the nearest and the brightest millisecond pulsar PSR J0437-4715 was published by the NICER collaboration [66]. The new data matches well with our results at the 90% CI. Hence, we have not incorporated it into our analysis. However, we plan to conduct a thorough study to quantify the effect of the new data.

ACKNOWLEDGEMENTS

This work has been partially supported by the Fonds de la Recherche Scientifique-FNRS, Belgium, under grant No. 4.4501.19. PC is supported by European Union's HORIZON MSCA-2022-PF-01-01 Pro-

gramme under Grant Agreement No. 101109652, project ProMatEx-NS. BB acknowledges the support from the

Deutsche Forschungsgemeinschaft (DFG, German Research Foundation) under Germany's Excellence Strategy – EXC 2121 “Quantum Universe” – 390833306.

-
- [1] V. Doroshenko, V. Suleimanov, G. Pühlhofer, and A. Santangelo, *Nature Astronomy* **6**, 1444 (2022).
- [2] L. Brodie and A. Haber, *Phys. Rev. C* **108**, 025806 (2023), arXiv:2302.02989 [nucl-th].
- [3] K. Huang, H. Shen, J. Hu, and Y. Zhang, *Phys. Rev. D* **109**, 043036 (2024), arXiv:2306.04992 [nucl-th].
- [4] J. J. Li and A. Sedrakian, *Phys. Lett. B* **844**, 138062 (2023), arXiv:2306.14185 [nucl-th].
- [5] S. Kubis, W. Wójcik, D. A. Castillo, and N. Zabari, *Phys. Rev. C* **108**, 045803 (2023), arXiv:2307.02979 [nucl-th].
- [6] H. Koehn *et al.*, (2024), arXiv:2402.04172 [astro-ph.HE].
- [7] Z. Miao, L. Qi, J. Zhang, A. Li, and M. Ge, *Phys. Rev. D* **109**, 123005 (2024), arXiv:2402.02799 [astro-ph.HE].
- [8] F. Di Clemente, A. Drago, and G. Pagliara, *Astrophys. J.* **967**, 159 (2024), arXiv:2211.07485 [astro-ph.HE].
- [9] J. E. Horvath, L. S. Rocha, L. M. de Sá, P. H. R. S. Moraes, L. G. Barão, M. G. B. de Avellar, A. Bernardo, and R. R. A. Bacheaga, *Astron. Astrophys.* **672**, L11 (2023), arXiv:2303.10264 [astro-ph.HE].
- [10] P. T. Oikonomou and C. C. Moustakidis, *Phys. Rev. D* **108**, 063010 (2023), arXiv:2304.12209 [astro-ph.HE].
- [11] I. A. Rather, G. Panotopoulos, and I. Lopes, *Eur. Phys. J. C* **83**, 1065 (2023), arXiv:2307.03703 [astro-ph.HE].
- [12] W.-L. Yuan and A. Li, *Astrophys. J.* **966**, 3 (2024), arXiv:2312.17102 [nucl-th].
- [13] M. Mariani, I. F. Ranea-Sandoval, G. Lugones, and M. G. Orsaria, (2024), arXiv:2407.06347 [astro-ph.HE].
- [14] V. Sagun, E. Giangrandi, T. Dietrich, O. Ivanytskyi, R. Negreiros, and C. Providência, *Astrophys. J.* **958**, 49 (2023), arXiv:2306.12326 [astro-ph.HE].
- [15] N. K. Glendenning, *Compact stars: Nuclear physics, particle physics, and general relativity* (New York, USA: Springer, 390 p, 1997).
- [16] J. A. J. Alford and J. P. Halpern, *Astrophys. J.* **944**, 36 (2023), arXiv:2302.05893 [astro-ph.HE].
- [17] J. Antoniadis *et al.*, *Science* **340**, 6131 (2013), arXiv:1304.6875 [astro-ph.HE].
- [18] H. T. Cromartie *et al.*, *Nature Astron.* **4**, 72 (2019), arXiv:1904.06759 [astro-ph.HE].
- [19] E. Fonseca *et al.*, *Astrophys. J. Lett.* **915**, L12 (2021), arXiv:2104.00880 [astro-ph.HE].
- [20] B. P. Abbott *et al.* (LIGO Scientific, Virgo), *Phys. Rev. Lett.* **119**, 161101 (2017), arXiv:1710.05832 [gr-qc].
- [21] B. P. Abbott *et al.* (LIGO Scientific, Virgo, Fermi GBM, INTEGRAL, IceCube, AstroSat Cadmium Zinc Telluride Imager Team, IPN, Insight-Hxmt, ANTARES, Swift, AGILE Team, 1M2H Team, Dark Energy Camera GW-EM, DES, DLT40, GRAWITA, Fermi-LAT, ATCA, ASKAP, Las Cumbres Observatory Group, OzGrav, DWF (Deeper Wider Faster Program), AST3, CAASTRO, VINROUGE, MASTER, J-GEM, GROWTH, JAGWAR, CaltechNRAO, TTU-NRAO, NuSTAR, Pan-STARRS, MAXI Team, TZAC Consortium, KU, Nordic Optical Telescope, ePESSTO, GROND, Texas Tech University, SALT Group, TOROS, BOOTES, MWA, CALET, IKI-GW Follow-up, H.E.S.S., LOFAR, LWA, HAWC, Pierre Auger, ALMA, Euro VLBI Team, Pi of Sky, Chandra Team at McGill University, DFN, ATLAS Telescopes, High Time Resolution Universe Survey, RIMAS, RATIR, SKA South Africa/MeerKAT), *Astrophys. J. Lett.* **848**, L12 (2017), arXiv:1710.05833 [astro-ph.HE].
- [22] T. E. Riley *et al.*, *Astrophys. J. Lett.* **887**, L21 (2019), arXiv:1912.05702 [astro-ph.HE].
- [23] M. C. Miller *et al.*, *Astrophys. J. Lett.* **887**, L24 (2019), arXiv:1912.05705 [astro-ph.HE].
- [24] T. E. Riley *et al.*, *Astrophys. J. Lett.* **918**, L27 (2021), arXiv:2105.06980 [astro-ph.HE].
- [25] M. C. Miller *et al.*, *Astrophys. J. Lett.* **918**, L28 (2021), arXiv:2105.06979 [astro-ph.HE].
- [26] D. Adhikari *et al.* (PREX), *Phys. Rev. Lett.* **126**, 172502 (2021), arXiv:2102.10767 [nucl-ex].
- [27] D. Adhikari *et al.* (CREX), *Phys. Rev. Lett.* **129**, 042501 (2022), arXiv:2205.11593 [nucl-ex].
- [28] K. Hebeler, J. M. Lattimer, C. J. Pethick, and A. Schwenk, *Astrophys. J.* **773**, 11 (2013), arXiv:1303.4662 [astro-ph.SR].
- [29] I. Tews, T. Krüger, K. Hebeler, and A. Schwenk, *Phys. Rev. Lett.* **110**, 032504 (2013), arXiv:1206.0025 [nucl-th].
- [30] J. E. Lynn, I. Tews, J. Carlson, S. Gandolfi, A. Gezerlis, K. E. Schmidt, and A. Schwenk, *Phys. Rev. Lett.* **116**, 062501 (2016), arXiv:1509.03470 [nucl-th].
- [31] C. Drischler, K. Hebeler, and A. Schwenk, *Phys. Rev. C* **93**, 054314 (2016), arXiv:1510.06728 [nucl-th].
- [32] C. Drischler, K. Hebeler, and A. Schwenk, *Phys. Rev. Lett.* **122**, 042501 (2019), arXiv:1710.08220 [nucl-th].
- [33] S. Huth, C. Wellenhofer, and A. Schwenk, *Phys. Rev. C* **103**, 025803 (2021), arXiv:2009.08885 [nucl-th].
- [34] C. Drischler, J. W. Holt, and C. Wellenhofer, *Ann. Rev. Nucl. Part. Sci.* **71**, 403 (2021), arXiv:2101.01709 [nucl-th].
- [35] B. Biswas, P. Char, R. Nandi, and S. Bose, *Phys. Rev. D* **103**, 103015 (2021), arXiv:2008.01582 [astro-ph.HE].
- [36] B. Biswas, R. Nandi, P. Char, S. Bose, and N. Stergioulas, *Mon. Not. Roy. Astron. Soc.* **505**, 1600 (2021), arXiv:2010.02090 [astro-ph.HE].
- [37] B. Biswas, *Astrophys. J.* **921**, 63 (2021), arXiv:2105.02886 [astro-ph.HE].
- [38] T. Ghosh, B. Biswas, and S. Bose, *Phys. Rev. D* **106**, 123529 (2022), arXiv:2203.11756 [astro-ph.CO].
- [39] T. Ghosh, B. Biswas, S. Bose, and S. J. Kapadia, (2024), arXiv:2407.16669 [gr-qc].
- [40] B. A. Brown and A. Schwenk, *Phys. Rev. C* **89**, 011307 (2014), [Erratum: *Phys. Rev. C* **91**, 049902 (2015)], arXiv:1311.3957 [nucl-th].
- [41] J. Margueron, R. Hoffmann Casali, and F. Gulminelli, *Phys. Rev. C* **97**, 025805 (2018), arXiv:1708.06894 [nucl-th].
- [42] C. Y. Tsang, B. A. Brown, F. J. Fattoyev, W. G. Lynch, and M. B. Tsang, *Phys. Rev. C* **100**, 062801 (2019), arXiv:1908.11842 [nucl-th].

- [43] M. Oertel, M. Hempel, T. Klöhn, and S. Typel, *Rev. Mod. Phys.* **89**, 015007 (2017), arXiv:1610.03361 [astro-ph.HE].
- [44] M. Dutra, O. Lourenco, J. S. Sa Martins, A. Delfino, J. R. Stone, and P. D. Stevenson, *Phys. Rev. C* **85**, 035201 (2012), arXiv:1202.3902 [nucl-th].
- [45] M. Dutra, O. Lourenço, S. S. Avancini, B. V. Carlson, A. Delfino, D. P. Menezes, C. Providência, S. Typel, and J. R. Stone, *Phys. Rev. C* **90**, 055203 (2014), arXiv:1405.3633 [nucl-th].
- [46] J. S. Read, B. D. Lackey, B. J. Owen, and J. L. Friedman, *Phys. Rev. D* **79**, 124032 (2009), arXiv:0812.2163 [astro-ph].
- [47] G. Baym, C. Pethick, and P. Sutherland, *Astrophys. J.* **170**, 299 (1971).
- [48] J. Aasi *et al.* (LIGO Scientific), *Class. Quant. Grav.* **32**, 074001 (2015), arXiv:1411.4547 [gr-qc].
- [49] F. Acernese *et al.* (VIRGO), *Class. Quant. Grav.* **32**, 024001 (2015), arXiv:1408.3978 [gr-qc].
- [50] B. P. Abbott *et al.* (LIGO Scientific, Virgo), *Phys. Rev. X* **9**, 011001 (2019), arXiv:1805.11579 [gr-qc].
- [51] B. Abbott *et al.* (LIGO Scientific, Virgo), *Astrophys. J. Lett.* **892**, L3 (2020), arXiv:2001.01761 [astro-ph.HE].
- [52] T. E. Riley, A. L. Watts, S. Bogdanov, P. S. Ray, R. M. Ludlam, S. Guillot, Z. Arzoumanian, C. L. Baker, A. V. Bilous, D. Chakrabarty, K. C. Gendreau, A. K. Harding, W. C. G. Ho, J. M. Lattimer, S. M. Morsink, and T. E. Strohmayer, “*A NICER View of PSR J0030+0451: Nested Samples for Millisecond Pulsar Parameter Estimation*,” (2019).
- [53] T. E. Riley, A. L. Watts, P. S. Ray, *et al.*, “*A NICER View of the Massive Pulsar PSR J0740+6620 Informed by Radio Timing and XMM-Newton Spectroscopy: Nested Samples for Millisecond Pulsar Parameter Estimation*,” (2021).
- [54] M. C. Miller, F. K. Lamb, A. J. Dittmann, S. Bogdanov, Z. Arzoumanian, K. C. Gendreau, S. Guillot, A. K. Harding, W. C. G. Ho, J. M. Lattimer, R. M. Ludlam, S. Mahmoodifar, S. M. Morsink, P. S. Ray, T. E. Strohmayer, K. S. Wood, T. Enoto, R. Foster, T. Okajima, G. Prigozhin, and Y. Soong, “NICER PSR J0030+0451 Illinois-Maryland MCMC Samples,” (2019).
- [55] M. Miller, F. K. Lamb, A. J. Dittmann, *et al.*, “NICER PSR J0740+6620 Illinois-Maryland MCMC Samples,” (2021).
- [56] V. Doroshenko, V. F. Suleimanov, G. Pühlhofer, and A. Santangelo, “MCMC samples for X-ray spectra fits summarised in the paper ”A strangely light neutron star”,” (2022).
- [57] G. Raaijmakers *et al.*, *Astrophys. J. Lett.* **893**, L21 (2020), arXiv:1912.11031 [astro-ph.HE].
- [58] R. Essick, I. Tews, P. Landry, and A. Schwenk, (2021), arXiv:2102.10074 [nucl-th].
- [59] X. Viñas, M. Centelles, X. Roca-Maza, and M. Warda, *Eur. Phys. J. A* **50**, 27 (2014), arXiv:1308.1008 [nucl-th].
- [60] S. K. Tripathy, D. Behera, T. R. Routray, and B. Behera, (2020), arXiv:2009.00427 [nucl-th].
- [61] B. T. Reed, F. J. Fattoyev, C. J. Horowitz, and J. Piekarewicz, *Phys. Rev. Lett.* **126**, 172503 (2021), arXiv:2101.03193 [nucl-th].
- [62] B. T. Reed, F. J. Fattoyev, C. J. Horowitz, and J. Piekarewicz, *Phys. Rev. C* **109**, 035803 (2024), arXiv:2305.19376 [nucl-th].
- [63] H. D. Thi, C. Mondal, and F. Gulminelli, *Universe* **7**, 373 (2021), arXiv:2109.09675 [astro-ph.HE].
- [64] C. Mondal and F. Gulminelli, *Phys. Rev. C* **107**, 015801 (2023), arXiv:2209.05177 [nucl-th].
- [65] P. Char, C. Mondal, F. Gulminelli, and M. Oertel, *Phys. Rev. D* **108**, 103045 (2023), arXiv:2307.12364 [nucl-th].
- [66] D. Choudhury *et al.*, *Astrophys. J. Lett.* **971**, L20 (2024), arXiv:2407.06789 [astro-ph.HE].